

pubs.acs.org/acscatalysis Research Article

# Mechanistic Insight into Cu-Catalyzed C-N Coupling of Hindered Aryl Iodides and Anilines Using a Pyrrol-ol Ligand Enables Development of Mild and Homogeneous Reaction Conditions

Antoine de Gombert, Andrea Darù, Tonia S. Ahmed, Michael C. Haibach, Rei Li-Matsuura, Cassie Yang, Rodger F. Henry, Silas P. Cook,\* Shashank Shekhar,\* and Donna G. Blackmond\*



Cite This: ACS Catal. 2023, 13, 2904-2915



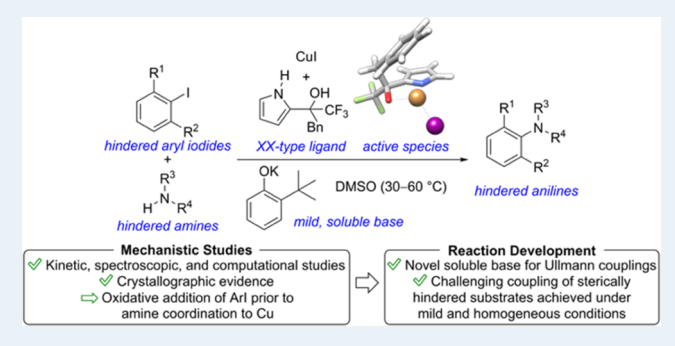
**ACCESS** I

III Metrics & More

Article Recommendations

Supporting Information

ABSTRACT: Mechanistic studies of the Cu-catalyzed C-N coupling of sterically hindered aryl iodides with sterically hindered anilines are carried out to shed light on how a recently reported pyrrol-ol ligand affects the reaction. Kinetic, spectroscopic, and computational tools help to probe the nature of the active catalyst species and the rate-determining step in the cycle. In contrast to most known Cu systems, oxidative addition is found to precede coordination of the amine. These studies help to design an efficient process under mild conditions using a fully homogeneous system as well as protocols that enable high yields by temperature scanning and controlled addition of the base. The insights obtained for the XX-type ligand may lead to a general approach for challenging substrate classes in Cu-catalyzed coupling reactions.



KEYWORDS: C-N coupling, kinetics, Cu catalysis, catalytic mechanisms, sterically hindered substrates

#### **■ INTRODUCTION**

Transition-metal-catalyzed C-N coupling reactions have become a key tool in organic synthesis, with applications in pharmaceuticals, material, and natural product synthesis. The Pd-catalyzed Buchwald-Hartwig reaction is one of the best studied and most effective means of carrying out these couplings,<sup>2,3</sup> although Cu catalysis has also proven to be successful in, for example, Ullmann-Goldberg reactions.<sup>4-6</sup> While Cu has a significant advantage over Pd in terms of cost, lower toxicity, and environmental impact, Cu catalysis has lagged behind in terms of both the substrate scope and mechanistic understanding. One of the major limitations of Cucatalyzed methods is their inability to couple sterically hindered partners. 8-12 Some of us recently reported that a novel pyrrol-ol ligand 4 (Scheme 1a), discovered by screening of ligand-like structures in AbbVie's internal compound library followed by optimization, enables Cu-catalyzed reactions between a wide variety of ortho and ortho, ortho'-substituted aryl iodides and hindered primary aliphatic amines, anilines, and amides such as product 3a. 13 Despite significant advancement in the Cucatalyzed Ullmann-Goldberg method, this reaction requires high temperatures, an insoluble base, molecular sieves, and a stoichiometric amount of Hantzsch ester, conditions that can impede its use in large-scale applications. In addition, catalyst deactivation due to ligand decomposition was noted under high temperatures. No mechanistic study was reported, although it

was suggested that the ligand would be either mono (LX-type)or bis-deprotonated (XX-type) under reaction conditions in a complex formed with Cu.

The current work reports a detailed mechanistic study of the reaction in Scheme 1b, enlisting kinetic, spectroscopic, and computational tools to provide insights into the reaction mechanism and the nature of this novel catalyst. These findings led to the development of significantly milder (30–60 °C) and fully homogeneous reaction conditions using a mild base, potassium 2-tert-butylphenoxide, in the absence of any additive (Scheme 1b). Most Cu-catalyzed amination reactions are conducted under heterogeneous conditions with inorganic bases such as  $K_3PO_4$  or  $Cs_2CO_3$ . Inadequate suspension of insoluble bases in organic solvents may lead to irreproducible observations during large-scale applications. <sup>14,15</sup> Only a few examples of homogeneous Cu-catalyzed amination either in the presence of ionic <sup>16–18</sup> or strong alkoxide bases <sup>9,19</sup> are known. We disclose a convenient and scale-friendly method using an inexpensive and readily prepared soluble base with unprece-

Received: December 15, 2022 Revised: January 20, 2023 Published: February 10, 2023





#### Scheme 1. Cu-Catalyzed C-N Coupling

#### (a) Previous reaction conditions

#### **Advantages**

- Novel ligand scaffold
- · Unprecedented scope for sterically hindered coupling partners
- Coupling of amines with N-H p $K_a$  range of ~ 20 to ~ 40

#### **Disadvantages**

- Heterogeneous reaction conditions and additives can impede applications on large-scale
- High reaction temperature leads to ligand decomposition

#### (b) Current work

kinetic, spectroscopic, structural and computational studies

Mechanistic understanding: unusual 'aryl-iodide first' pathway for Cu-catalyzed C-N coupling

dented substrate scope for Cu-catalyzed amination reactions under mild conditions. The nature of the active catalyst species and the dynamic role of the soluble base in establishing the active catalyst are highlighted.

We demonstrate that 4 chelates Cu in a  $\kappa^2_{N,O}$  fashion via both deprotonated N and O atoms simultaneously, therefore acting as an XX-type ligand for Cu, as opposed to ligands such as bipyridines/phenanthrolines (LL-type) or 2-picolinic acid/1,3-dicarbonyls (LX-type). In contrast with most Cu-catalyzed N-arylation reactions,  $^{17,20-26}$  our results indicate that oxidative addition of aryl iodide precedes coordination of the amine to this low-valent Cu(I) chelate and that this step is the rate-determining step. The sequence of oxidative addition followed by amine coordination to Cu is reminiscent of the typical mechanism of Pd-catalyzed amination reactions. Perhaps the discovery of other XX-type ligands will render Cu-catalyzed methods tolerant to steric properties of reactants as some of the Pd-catalyzed methods.

#### ■ RESULTS AND DISCUSSION

Preliminary kinetic studies testing various reaction conditions led to improvements including removal of molecular sieves, decrease in the amount of Hantzsch ester, and most importantly, a significant decrease in the reaction temperature from 90 to 60 °C. As shown in Figure 1, the reaction of Scheme 1b under these conditions monitored by reaction calorimetry and validated by discrete NMR sampling revealed an unusual kinetic profile, with a rapid initial conversion followed by a slower rate. Using 10 mol % catalyst, the reaction achieves over 50% conversion in less than 2 h and eventually gives quantitative yield. Under these lower temperature conditions, no ligand decomposition was observed.

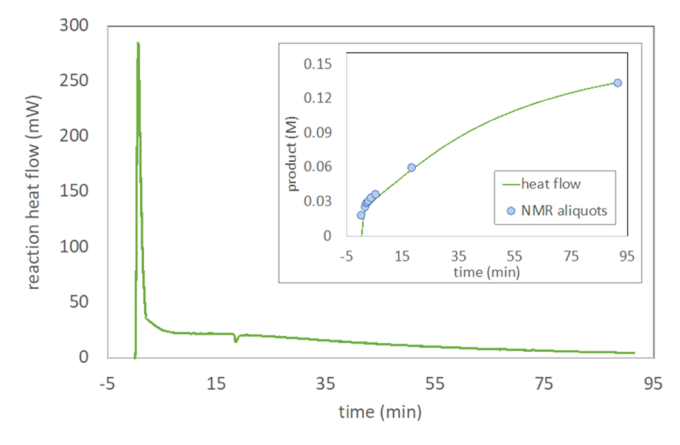


**Figure 1.** Product concentration vs time for the reaction of Scheme 1b under modified conditions: 0.25 M **1a**, 0.425 M **2a**, 10 mol % CuI/4, 0.05 M Hantzsch ester, 4 equiv K<sub>3</sub>PO<sub>4</sub>, 60 °C in dimethyl sulfoxide (DMSO). Reaction rate monitored by calorimetry (green curve); inset: temporal heat flow integrated to give product **3a** concentration (green line), verified by NMR sampling (blue circles).

Further kinetic studies using a novel temperature scanning reaction (TSR) protocol<sup>34,35</sup> showed that the initial burst of high reactivity occurs even at ambient temperature (Figure 2). Ramping the temperature after this initial activity provides high conversion in a few hours and yields the Arrhenius plot shown in the inset of Figure 2. The maximum rate of this initial burst appears to reach a plateau as a function of increasing catalyst concentration, as shown in Figure 3. Such a plateau indicates that a process other than the catalytic reaction step is controlling the rate.

These findings suggest that the reaction becomes limited by the rate of transfer of the insoluble base (K<sub>3</sub>PO<sub>4</sub>) into solution,

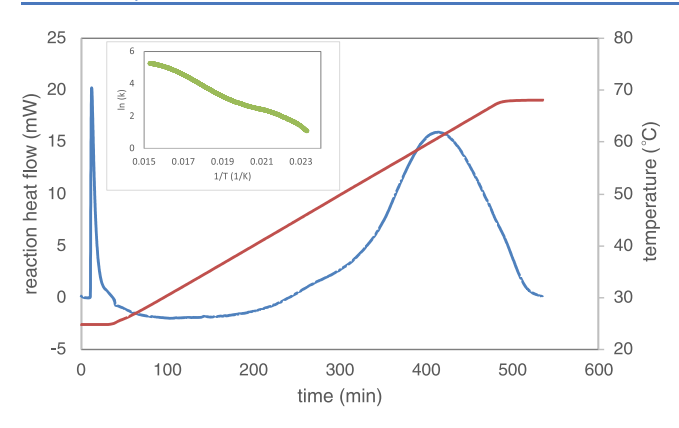


**Figure 2.** Temperature scanning protocol for the reaction of Scheme 1b carried out under the conditions of Figure 1 beginning at 25  $^{\circ}$ C and scanning at a rate of 0.1  $^{\circ}$ C/min. Inset shows an Arrhenius plot of the data obtained during the temperature ramp.

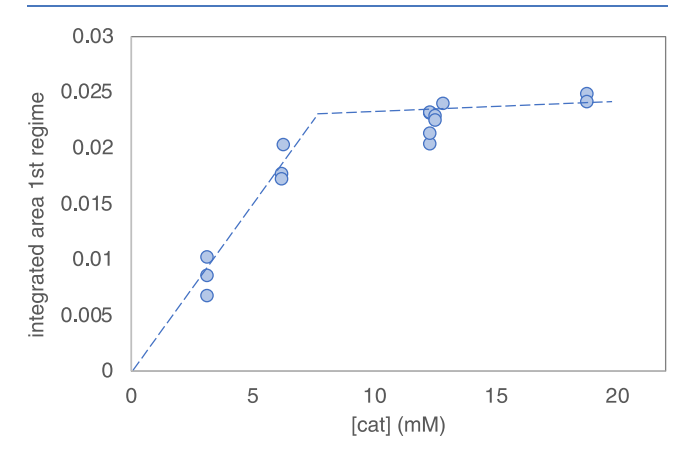


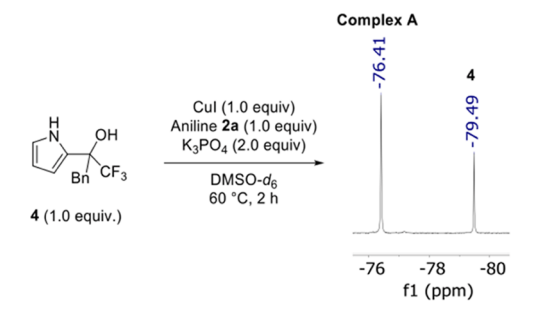
**Figure 3.** Plot of conversion obtained in the initial rapid rate burst as a function of Cu loading in the reaction of 1a with 2a and CuI/4 at  $60\,^{\circ}$ C in DMSO, with various concentrations of catalyst loading as shown. See the Supporting Information for full experimental details. Product concentration calculated from the area under the heat flow curve for the first regime, which gives the heat of reaction for the number of moles of product formed. Lines are drawn as a guide to the eye.

which decreases the reaction efficiency and hinders the study of the intrinsic reaction kinetics. This led to the screening of soluble bases (Scheme 2), which revealed that a number of phenolate-type bases affect the reaction at ambient temperature, <sup>36–41</sup> with varying degrees of efficiency. Under these

conditions, the reactions were run without Hantzsch ester since it was found that the yield was similar in its absence. The strongly hindered bases 5 and 6 formed 3a in a low but detectable yield. While 2,6-di-t-Bu phenolate 7 also formed the product in low yield, the less sterically hindered phenolate 8 and a slightly more electron-donating base 9 (compared to 8) gave much-improved yields of product 3a. Interestingly, base 10, an electron-deficient analogue of 9, did not lead to product formation. Potassium 2-tert-butylphenoxide (7) readily prepared from widely available and inexpensive 2-tert-butylphenol was chosen for further studies. This study shows that homogeneous phenolate bases provide another vector of optimization for this coupling reaction. In contrast to the phenolate bases, soluble amine bases, and KO¹Bu were not competent in the reaction.

The use of a soluble base also facilitates studies aimed at understanding the active catalyst species formed between Cu and ligand 4 in the reaction. In preliminary  $^{19}F$  NMR studies of the stoichiometric interaction between CuI and ligand 4 in the presence of aniline 2a and  $K_3PO_4$  at 60 °C, a new species, complex A, was observed along with free ligand 4 (Scheme 3).

Scheme 3. Formation of Intermediate Species between CuI and Ligand 4



Complex **A** was not observed in the absence of the base, as dissolution of CuI and 4 in DMSO- $d_6$  did not cause any change in the  $^1\text{H}$  and  $^{19}\text{F}$  NMR resonance peaks of 4, even after heating the reaction mixture at 60 °C. In contrast, complex **A** was observed when CuI was added to a pre-stirred solution of 4 and KH in DMSO. Complex **A** was formed in ca. 1:1 ratio with ligand 4 and was therefore attributed to an anionic  $\kappa^2_{\text{N,O}}$  chelated Cu(I) structure (Scheme 4a). Complex **A** was also formed in similar proportions when CuI and 4 were reacted with 1 equiv of base **9** (Scheme 4b). Increasing the number of equivalents of

Scheme 2. Screening of Soluble Bases in the Reaction of Scheme 1b at Low Temperature

#### Scheme 4. Formation of Complexes A and B

(a) Formation of a bis anionic-Cu(I) complex, complex  ${\bf A}$ , in the presence of a non-coordinating base, KH

(b) Formation of complex A, in the presence of base 9

(c) Formation of 2-tert-butylphenoxyde bound bis anionic Cu-complex, complex B

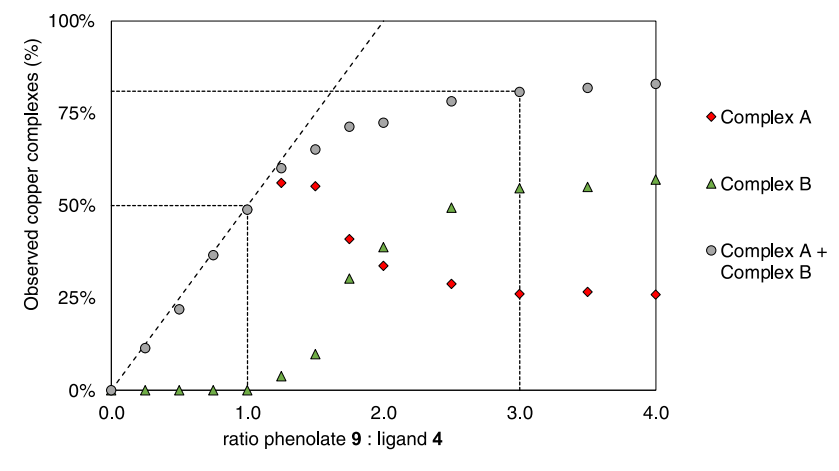


**Figure 4.** Formation of complexes **A** and **B** by addition of increasing concentrations of base **9** to equimolar solutions of CuI and ligand **4.** Dotted lines: 4/A/B = 50:50:0 when 9/4 = 1:1, corresponding to Scheme 4b. 4/A/B = 19:26:55 when 9/4 = 3:1, corresponding to Scheme 4c.

base 9 did not improve the yield of complex A. Instead, the formation of a novel species (complex B) in which 2-tert-butylphenoxide has replaced the iodide in complex A, was observed (Scheme 4c).

The formation of complexes **A** and **B** was further investigated by <sup>1</sup>H and <sup>19</sup>F NMR spectroscopy in the presence of 0–4 equiv of base **9** (Figure 4). A monotonic increase in the formation of complex **A** was observed upon the addition of up to 1 equiv of **9** to stoichiometric concentrations of CuI and **4**. During this linear increase, 2 equiv of **9** were required for the formation of each equivalent of complex **A**, supporting the proposal that complex **A** is a Cu complex, in which both the amine and hydroxyl protons of **4** have been deprotonated. At higher equivalents of **9**, complex **B** becomes the major compound.

The assigned structures of complexes **A** and **B** were supported by isolation of related Cu complexes as well as density functional

theory (DFT) calculations (Scheme 5). The reaction of copper mesitylene with 4 and potassium tert-butoxide in tetrahydrofuran (THF), followed by diffusion of a [2.2.2]-cryptand THF solution formed a dimeric Cu complex (Cu-dimer, Scheme 5a), as determined by X-ray crystallography. Such a structure confirms that 4 can lead to ionic Cu(I) complexes by binding copper simultaneously through its nitrogen and oxygen atoms in an anionic X-type fashion. Another Cu complex (complex B', Scheme 5b) was isolated from the reaction of copper mesitylene with 4 and 9, followed by diffusion of a [2.2.2]-cryptand THF. In complex B', 9 and the deprotonated nitrogen atom of 4 are coordinated to Cu and the oxygen atom of 4 is present as OH. Both Cu-dimer and complex B' catalyzed the reaction shown in Scheme 1b. This shows their relevance to the reaction mechanism and suggests that both proceed via a common reactive intermediate, presumably complex A.<sup>42</sup>

Scheme 5. (a, b) Isolation of Cu-Dimer and Complex B' and Their Crystal Structures; (c, d) Graphical Representations of Complexes A and B (OAr" = 2-tert-Butylphenoxide)

<sup>a</sup>The solid-state structures are represented with thermal ellipsoids at a 50% probability level. K[2.2.2-cryptand] units are omitted for clarity. <sup>b</sup>Solvent molecules are shown in a slimmer fashion for clarity. Cu: orange; I: purple; K: violet; S: yellow; F: light green; C: gray; O: red; N: blue; H: white.

As attempts to isolate complexes A and B remained unsuccessful, their structures were studied computationally.

The structure of complex **A** can be described as an ion pair, with CuI coordinated to the bis-deprotonated ligand **4** (Scheme 5c). The phenyl ring of **4** is located on the upper side of the complex. The nearest C=C bond of the phenyl ring is at a distance of 3 Å from the Cu center, and although this is in the range of a standard  $\pi$ -stacking, no overlap of the molecular orbitals of the structure is observed. Below the ligand plane, two K<sup>+</sup> cations interact with both the ligand and Cu, while surrounded by a total of five DMSO molecules. Similarly, the optimized structure of complex **B** was obtained, which shows the same structural features as **A** in addition to the presence of 2-tert-butylphenoxide instead of iodide.

In stoichiometric reaction studies, the coupled product 3a was observed in 80% yield when complex A, generated *in situ* from the reaction of equimolar amounts of CuI, 4, and 9 was subjected to 2 equiv each of 1a and 2a, indicating that complex A is competent to mediate the reaction (Scheme 6a). No change in the  $^{19}F$  NMR signal of complex A was observed when aniline 2a (2 equiv) was treated with complex A in DMSO- $d_6$ , indicating that complex A does not interact with aniline in the absence of aryl iodide (Scheme 6b). In contrast, aryl iodide reacts readily with complex A in the absence of aniline. For example, complex A reacted with 1-fluoro-4-iodobenzene (2 equiv) to form fluorobenzene, 4,4'-difluoro-1,1'-biphenyl, arylated base and ligand (Scheme 6c), as determined by mass spectrometry and NMR spectroscopy.

Under catalytic reaction conditions, the base is present in large excess over the catalyst. Figure 5 shows that under a 10-fold excess of base 9 in the presence of equimolar CuI and 4, the signals for complexes A and B become broad and overlap, with complex B appearing to dominate. Other unidentified species are also formed. These species disappear upon addition of increasing amounts of 2-tert-butylphenol (9-OH) to the solution, and the concentration of the combined complexes A

#### Scheme 6. Interaction of Complex A with Reaction Partners<sup>a</sup>

(a) Stoichiometric reaction of complex A with aryl iodide 1a and aniline 2a

(b) Stoichiometric reaction of complex A with aniline 2a

Complex A 
$$2a (2.0 \text{ equiv})$$
 No change in complex A NMR signals

 $(\boldsymbol{c})$  Stoichiometric reaction of complex  $\boldsymbol{A}$  with aryl iodide  $\boldsymbol{1}\text{-}\boldsymbol{F}$ 

<sup>a</sup>Complex A was generated in situ from a solution of CuI (0.025 mmol, 1.0 equiv), 4 (0.025 mmol, 1.0 equiv), and 9 (0.025 mmol, 1.0 equiv) in DMSO- $d_6$ .

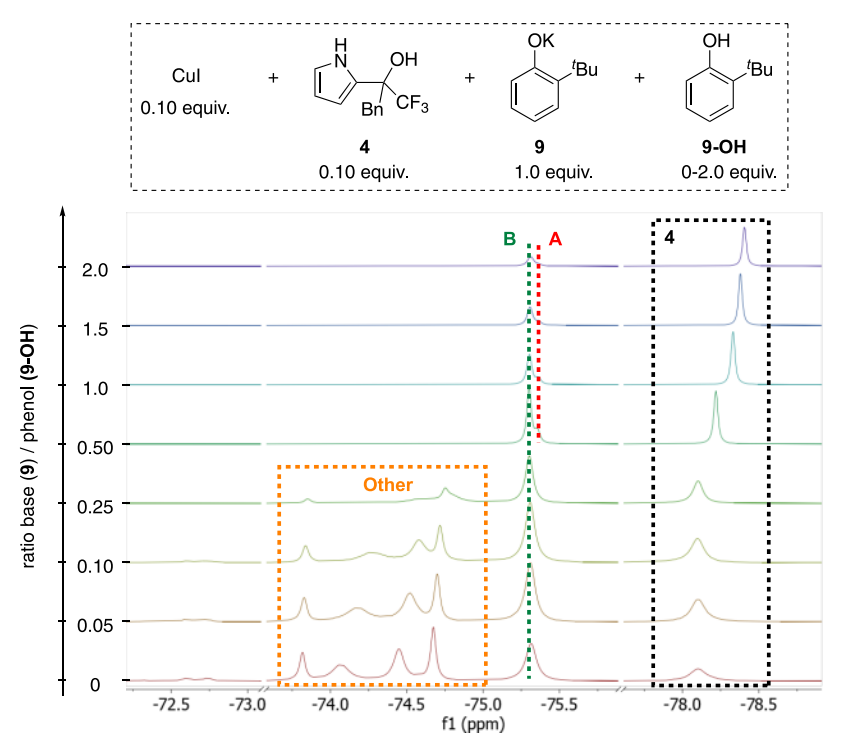


**Figure 5.** <sup>19</sup>F NMR signals for free ligand 4, complex **A**, complex **B**, and other species formed in the presence of equimolar amounts of CuI and 4 and a 10-fold excess of base **9** (bottom spectrum) and increasing amounts of the phenol **9-OH** (ascending spectra).

and B decreases while the concentration of free ligand 4 increases.

If complex A is an active catalyst species, as these results suggest, then maximizing its concentration is the key to high reactivity. This in turn requires a balance between having a sufficient base to drive the reaction of CuI and 4 toward complex A, but not a sufficient excess of 9 to push the reaction too far toward complex B or other inactive species, or a surfeit of 9-OH to drive the reaction toward free ligand 4 and inactive Cu complexes that we describe computationally (see below and Supporting Information). Finding this balance in the catalytic system is further complicated by the fact that the base is involved not only in the formation of the active catalyst but is also a stoichiometric reactant. At the beginning of the reaction, the Culigand complexes may partition as shown in the bottom spectrum of Figure 5, while later in the reaction, as the phenol 9-OH is formed in increasing amounts, the system may resemble the spectra shown in the top spectrum of Figure 5. We reasoned that an optimum amount of phenol 9-OH added at the outset of the reaction might help to hinder the formation of the unidentified species and promote a higher concentration of complex A and therefore increased reactivity, while too little or too much phenol 9-OH should decrease reactivity. This hypothesis was borne out, as shown in Figure 6, when the addition of 1.0 equiv of 9-OH with respect to 9 was shown to provide the optimal reaction rate.

Catalytic reaction conditions were developed to maximize the concentration of complex A and to minimize formation of the aryl ether by-product, derived from the coupling of 9 with aryl iodide (Figure 7). The reaction of an aniline (1 equiv) and an aryl iodide (1.5 equiv) was initiated with CuI (10 mol %), 4 (12 mol %), 9-OH (0.2 equiv), and 9 (0.2 equiv) in DMSO at 30 °C, followed by the slow addition of a solution of 9 (1.8 equiv) in DMSO. While initiating the reaction with equimolar amounts of 9-OH and 9 ensured optimal concentration of A, slow addition

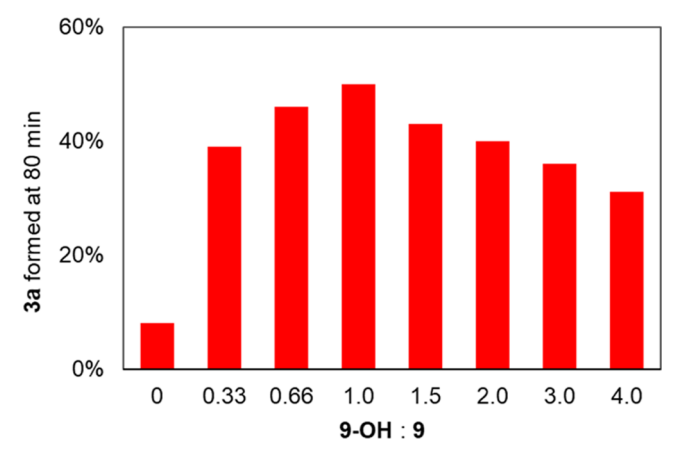


**Figure 6.** Product **3a** % at 80 min reaction time carried out with increasing amounts of the **9-OH** for the reaction shown in Scheme 1b.  $[1a]_0 = 100 \text{ mM}; [2a]_0 = 120 \text{ mM}; [9]_0 = 150 \text{ mM}; [CuI] = [4] = 10 \text{ mM}; 45 °C in DMSO under N<sub>2</sub>. Equivalents of the phenol$ **9-OH**added as shown.

of 9 avoided accumulation of the base, resulting in lower amounts of the aryl ether by-product. Unprecedented substrate scope was observed for Cu-catalyzed coupling of sterically hindered partners under mild and homogeneous conditions (Figure 7). 2-Iodotoluene 1a afforded the coupled products in excellent yields with a variety of 2- and 2,6-disubstituted anilines (3a, 11–15). Functional groups such as ester, nitrile, and ether were well tolerated (16–18). The mild reaction conditions allowed for the preferential C–N coupling of the hindered iodide in 4-bromo-1-iodo-2-methylbenzene (20–22) in >98:2 chemoselectivity. Mildly electron-deficient ArBr was also found to be a suitable electrophile (25), although a slightly higher temperature of 60 °C was required. Finally, 1a also coupled

Figure 7. Substrate scope under homogeneous reaction conditions (isolated yields). Unless noted otherwise, all reactions were conducted with amine (1.0 mmol), aryl iodide (1.5 mmol), CuI (0.1 mmol), 4 (0.12 mmol), 9-OH (0.2 mmol), and 9 (2 mmol) in DMSO (1 mL) at 30 °C for 16 h. (a) 60 °C. (b) Aryl iodide (1 mmol) and amine (1.5 mmol). (c) Aryl bromide was used as the electrophile.

efficiently with hindered primary and secondary amines (26–30).

Reaction progress kinetic analysis (RPKA) was performed to determine the concentration dependences of the substrates and catalyst as well as the robustness of the catalyst in the process (Figure 8). These studies were carried out under modified conditions, using a combination of 1.5 equiv of base 9 and 1.5 equiv of phenol 9-OH at the outset of the reaction to bypass the need for slow addition of the base. Time-adjusted plots of reactions designed with the "same excess" protocol showed overlay, indicating a lack of irreversible catalyst deactivation and a robust process (see the Supporting Information for details).

Varying the catalyst concentration shows that the reaction is first order in [Cu] (Figure 8, top). In "different excess" protocols, varying the concentration of aryl iodide 1a showed

first-order dependence on [1a] (Figure 8, middle), while reactions varying the concentration of aniline 2a gave identical rates (Figure 8, bottom). Figure 8 (bottom) also shows that reactions carried out with anilines 31 and 32 also gave rates identical to that observed with aniline 2a. In addition, the reaction rate is identical when other nucleophilic coupling partners, including 2-Ph-pyrrolidine 33, is employed. Zeroorder kinetics in both nucleophile concentration and identity, together with first order kinetics in [1a], points to a mechanism in which oxidative addition of the aryl iodide to the Cu catalyst is rate-determining and precedes the addition of aniline. These kinetic results indicate that this mechanism also holds for the secondary amine 33, even while a non-productive interaction between complex A and pyrrolidine 33 was observed. 43

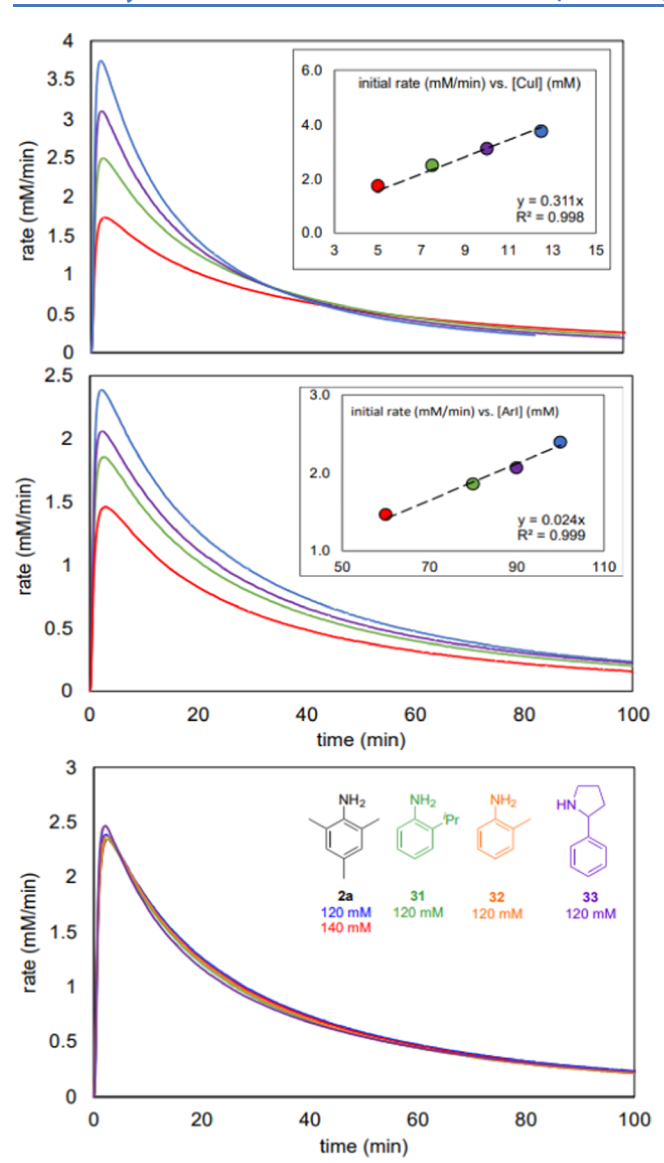


**Figure 8.** Kinetic studies of the reaction of Scheme 1 using soluble base 9 at 45 °C in DMSO under  $N_2$ . Standard conditions:  $[1a]_0 = 100$  mM;  $[2a]_0 = 120$  mM;  $[9]_0 = 150$  mM;  $[9-OH]_0 = 150$  mM; [CuI] = [4] = 10 mM. Top panel: rate vs time using different [CuI] = [4] as noted, middle panel: rate vs time using different  $[ArI]_0$  as noted; bottom panel: rate vs time using different  $[2a]_0$  and different nucleophiles and nucleophile concentrations as noted.

Radical clock experiments ruled out one-electron radical pathway for the reaction. <sup>44</sup> Together, these observations suggest the catalytic cycle proposed in Scheme 7. Oxidative addition of aryl iodide to complex A is turnover limiting and precedes the attack of the nucleophilic aniline (aryl halide first pathway), in contrast to other reported Cu-catalyzed coupling reactions, <sup>17,20–25,45</sup> where amine is proposed to interact with the catalyst prior to the oxidative addition with aryl halide (amine first pathway), but similar to Pd-catalyzed Buchwald—Hartwig cross-coupling reactions. The results from the stoichiometric experiments shown in Scheme 6 are also consistent with the aryl iodide first pathway because complex A did not interact with aniline but readily oxidatively added to aryl iodides in the absence of aniline.

Although the aryl halide first pathway for LX-type ligands has been proposed, no experimental evidence was provided. 46,47

Scheme 7. Proposed Catalytic Cycle for the Reaction of Scheme 1

Analogous to our proposed XX-type ligand 4, Davies and coworkers have reported that organic ionic base tetrabutylphosphonium malonate acts like a bis-anionic XX-type ligand for Cu; however, the amination reaction was reported to proceed via the amine first pathway. 17,23 Sterically encumbered electrophiles and nucleophiles formed only trace amounts of products. 18,23 Amination reactions catalyzed by Cu complexes of pyrrole-2carboxylic acid, reported by Buchwald and co-workers, <sup>48,49</sup> may also proceed via XX-type Cu intermediates; however, sterically encumbered coupling partners are not competent in the reaction.  $^{50}$  It appears that the ionic Cu(I) complex formed with the XX-type ligand 4 (complex A), is sufficiently electronrich to undergo oxidative addition to hindered aryl halides without the assistance of an amine. This mechanistic feature may help to rationalize the success of ligand 4 in reactions with hindered electrophiles.

This mechanism is also supported by DFT calculations (Figure 9). Ground state and transition state structures were optimized using B3LYP-D3BJ.<sup>51,52</sup> TPSSh-D3BJ was used for relative energy and free energy calculations.<sup>53</sup> Both implicit (SMD)<sup>54</sup> and explicit solvation models are used to treat the DMSO solvent on every calculated species.<sup>55</sup>

In the presence of base 9, CuI coordinates readily to ligand 4 to generate the catalytically active resting state complex A in an exothermic and irreversible process with a free energy change of -25.1 kcal/mol (Figure 9). Complex A can coordinate with 1a, 2a, 9, and 9-OH to form II, IIa, B, and B', respectively with the release of a molecule of KI. One of the species, complex B', was isolated and characterized by X-ray crystallography (Scheme 5b). Other species were computationally described. The formation of IIa is endergonic with a free energy change of +3.7 kcal/mol. This free energy gap is not prohibitive to the formation of such species; however, other structures that can lead to the final product 3a, specifically the coordination of aryl

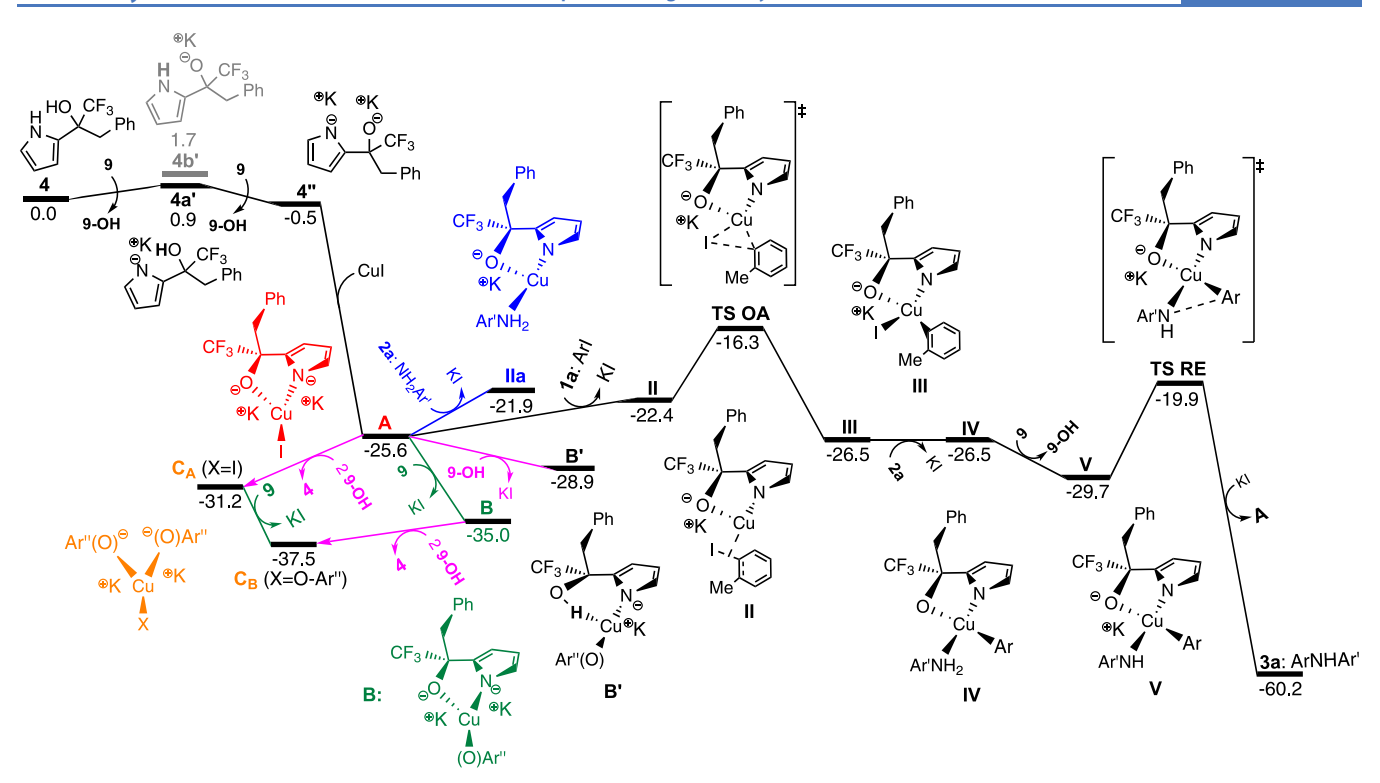


**Figure 9.** Free energy profile in kcal/mol of the suggested reaction mechanism computed at the TPSSh-D3BJ/**BBS** level of theory. All species drawn are calculated including explicit and implicit solvation herein removed for clarity (see Section S4.4 of the Supporting Information).

#### Scheme 8. Species Formed from CuI, Ligand 4, Base 9, and Phenol 9-OH

iodide 1a to IIa, could not be found. This is likely due to the steric bulk of 4 and the presence of  $K^+$  below the equatorial plane of the Cu center. The formation of II is also endergonic with a free energy change of +3.2 kcal/mol. II is the only species that can move forward to the further steps of the reaction. The activation free energy barrier for oxidative addition is low at 9.3 kcal/mol calculated from complex A, in agreement with the formation of the four products at room temperature described in Scheme 6c. The calculated oxidative addition complex III is located at -26.5 kcal/mol with a free energy change of -0.9 kcal/mol compared to complex A. III can now coordinate 2a

with concomitant release of KI in an isoenergetic step to form IV. This species contains both the molecules that are needed to form the final product through reductive elimination (RE). 9 exergonically deprotonates 2a coordinated to the Cu center in IV to generate V, which is 3.2 kcal/mol lower in free energy change compared to IV. IV undergoes reductive elimination crossing TS RE with 9.8 kcal/mol in activation free energy, releasing the final product 3a and regenerating complex A in an exergonic and irreversible step. The free energy change of the final step is -30.5 kcal/mol. At this point, complex A is ready to enter the catalytic cycle restarting the reaction. The reaction

coordinate presented in Figure 9 is in accordance with the kinetic results suggesting that oxidative addition of aryl iodide **1a** is the rate-determining step and precedes coordination of aniline in the productive catalytic cycle. A full free energy profile that also considers secondary pathways and reaction by-products is provided in the Supporting Information. <sup>57</sup>

Figure 6 demonstrates that the reaction is inhibited by excess of phenol 9-OH, which is also supported by the same excess protocol (see Section S2.5 in the Supporting Information for details).<sup>58</sup> Indeed, calculations show that an excess of conjugate acid 9-OH results in secondary processes; specifically, Scheme 8 shows that complexes A and B can react with 2 equiv of 9-OH to generate complexes C<sub>A</sub> and C<sub>B</sub>, respectively, and release ligand 4 in an exergonic process with free energy change of -5.6 and −2.5 kcal/mol, respectively, (see Section S4.2 in the Supporting Information for details). This is a re-protonation process of the ligand coordinated to complex A and B that were previously deprotonated by base 9. Experimentally, complex A, complex B, and ligand 4 (ca. 10:40:50 ratio) were the only species observed at the outset of the reaction. <sup>59</sup> The observation of free ligand 4 as the major species suggest that Cu is indeed sequestered as the inactive complex C<sub>B</sub> in the presence of excess base with respect to CuI. Complex A is the lowest energy on-cycle species, in equilibrium with the off-cycle resting state  $C_B$ . The activation free energy of the rate-determining oxidative addition step is 21.2 kcal/mol (Figure S18), in agreement with the kinetics observed at 45 °C. C<sub>A</sub> and C<sub>B</sub> present structures similar to complexes A and B: the Cu center coordinates two phenolate bases 9 at their O and at the same time two counterion K<sup>+</sup> are present surrounded by five DMSO molecules.<sup>60</sup>

#### CONCLUSIONS

Despite significant advances made in the Ullmann-Goldberg reaction, coupling sterically hindered partners remains a major limitation. To overcome this limitation and to further enhance the utility of Cu-catalyzed methods, mechanistic studies of the Cu-catalyzed C-N couplings of sterically hindered aryl iodides and anilines are carried out to shed light on how a novel pyrrol-ol ligand effects the reaction. In summary, we have developed mild and homogeneous conditions for coupling hindered aryl halides with hindered anilines and amines employing pyrrol-ol 4 as a ligand for Cu. The use of a hindered aryloxide base, potassium 2tert-butylpheoxide 9, was the key to the development of homogeneous conditions. Careful NMR studies revealed complex interaction of 9 and 9-OH with the active catalyst, resulting in catalyst deactivation and formation of an ether side product. Initiating the reaction with 1:1 ratio of 9 and 9-OH followed by slow addition of 9 prolonged the catalyst lifetime and allowed for a broad and unprecedented substrate scope for Cu-catalyzed methods.

The homogeneous conditions allowed us to conveniently conduct mechanistic studies using calorimetry and NMR spectroscopy. Ligand 4 acts as a XX-type ligand for Cu, generating a bis-anionic Cu complex (complex A). Complex A undergoes rate-limiting oxidative addition to aryl iodide prior to the coordination of amine, a key difference from the more precedented pathway where the amine coordination to Cu precedes the oxidative addition. We believe the bis-anionic complex A is sufficiently electron-rich to oxidatively add to even the hindered electrophiles. The resulting Cu(III) species III is able to coordinate to hindered anilines and amines, resulting in the formation of the coupled product. This pathway was well supported by computational studies. Prior to our discovery of

ligand 4, base metal-catalyzed preparation of bulky amines required alternative strategies such as those developed by the Baran<sup>61</sup> and Lalic<sup>62</sup> groups. Although powerful, these approaches are not as convenient and straightforward as coupling widely available aryl halides and amines. Thus, our initial report on the ability of ligand 4 to enable Cu-catalyzed coupling of sterically hindered aryl iodides and amines is a noteworthy advance. Since 4 was discovered via high throughput screening and not by rational design, there was no guidance for further reaction development. The mechanistic studies described here not only allowed us to develop homogeneous and mild reaction conditions for C-N coupling, but this work has also established a novel reaction mechanism for Cu-catalyzed C-N coupling using XX-type ligands. We have also identified catalyst deactivation pathways. We believe that the current study will spur identification of novel XX-type ligands to enable coupling of sterically hindered partners under mild conditions, significantly expanding the ability of Cucatalyzed methods to match the broad scope and generality of Pd-catalyzed methods. Studies on further exploring the core structure of 4 to identify additional XX-type ligands for coupling sterically hindered aryl bromides and chlorides with hindered N and O nucleophiles under homogeneous conditions and to avoid catalyst deactivation is ongoing in our laboratories.

#### ASSOCIATED CONTENT

#### Supporting Information

The Supporting Information is available free of charge at https://pubs.acs.org/doi/10.1021/acscatal.2c06201.

Details of general methods, kinetic, spectroscopic, crystallization, computational studies, and NMR spectra (PDF)

CIF file for the crystal structure of Complex B (CIF)

CIF file for the crystal structure of Cu-dimer (CIF)

#### AUTHOR INFORMATION

#### **Corresponding Authors**

Silas P. Cook – Department of Chemistry, Indiana University, Bloomington, Indiana 47405, United States; orcid.org/0000-0002-3363-4259; Email: sicook@indiana.edu

Shashank Shekhar — Process Research and Development, AbbVie Inc., North Chicago, Illinois 60064, United States; orcid.org/0000-0002-1903-5380; Email: shashankshekhar@abbvie.com

Donna G. Blackmond — Department of Chemistry, Scripps Research, La Jolla, California 92037, United States; orcid.org/0000-0001-9829-8375; Email: blackmond@scripps.edu

#### Authors

Antoine de Gombert — Department of Chemistry, Scripps Research, La Jolla, California 92037, United States Andrea Darù — Department of Chemistry, Scripps Research, La Jolla, California 92037, United States; orcid.org/0000-0002-0825-2101

Tonia S. Ahmed – Process Research and Development, AbbVie Inc., North Chicago, Illinois 60064, United States Michael C. Haibach – Process Research and Development,

AbbVie Inc., North Chicago, Illinois 60064, United States; o orcid.org/0000-0001-8383-5633

- Rei Li-Matsuura Department of Chemistry, Scripps Research, La Jolla, California 92037, United States; orcid.org/0000-0002-3334-6492
- Cassie Yang Process Research and Development, AbbVie Inc., North Chicago, Illinois 60064, United States; orcid.org/ 0000-0001-9194-9745

Rodger F. Henry – Process Research and Development, AbbVie Inc., North Chicago, Illinois 60064, United States

Complete contact information is available at: https://pubs.acs.org/10.1021/acscatal.2c06201

#### Notes

The authors declare no competing financial interest.

#### ACKNOWLEDGMENTS

D.G.B. acknowledges funding from the National Science Foundation under the GOALI program (Award Number:1955496) and from John C. Martin Endowed Chair at Scripps Research. AbbVie contributed to the design, approval, and execution of this study. T.S.A., M.C.H., and S.S. are current AbbVie employees and may own AbbVie stocks. S.C. acknowledges the NIH (GM121840) for partial support of this work.

#### REFERENCES

- (1) Kahl, T.; Schroder, K.-W.; Lawrence, F. R.; Marshall, W. J.; Hoke, H.; Jackh, R. *Ullmann's Encyclopedia of Industrial Chemistry*; Wiley-VCH: Weinheim, 2011; pp 465–478.
- (2) Ruiz-Castillo, P.; Buchwald, S. L. Applications of Palladium-Catalyzed C-N Cross-Coupling Reactions. *Chem. Rev.* **2016**, *116*, 12564–12649.
- (3) Hartwig, J. F.; Shaughnessy, K. H.; Shekhar, S.; Green, R. A. Palladium-Catalyzed Amination of Aryl Halides. In *Organic Reactions*; John Wiley & Sons, Inc., 2019; pp 853–958.
- (4) Yang, Q.; Zhao, Y.; Ma, D. Cu-Mediated Ullmann-Type Cross-Coupling and Industrial Applications in Route Design, Process Development, and Scale-up of Pharmaceutical and Agrochemical Processes. Org. Process Res. Dev. 2022, 26, 1690–1750.
- (5) Shaughnessy, K. H.; Ciganek, E.; DeVasher, R. B. Copper-Catalyzed Amination of Aryl and Alkenyl Electrophiles; Wiley: Weinheim, 2014; Vol. 85.
- (6) Evano, G.; Blanchard, N.; Toumi, M. Copper-Mediated Coupling Reactions and Their Applications in Natural Products and Designed Biomolecules Synthesis. *Chem. Rev.* **2008**, *108*, 3054–3131.
- (7) Bryan, M. C.; Dunn, P. J.; Entwistle, D.; Gallou, F.; Koenig, S. G.; Hayler, J. D.; Hickey, M. R.; Hughes, S.; Kopach, M. E.; Moine, G.; Richardson, P.; Roschangar, F.; Steven, A.; Weiberth, F. J. Key Green Chemistry research areas from a pharmaceutical manufacturers' perspective revisited. *Green Chem.* **2018**, *20*, 5082–5103.
- (8) Gao, J.; Bhunia, S.; Wang, K.; Gan, L.; Xia, S.; Ma, D. Discovery of N-(Naphthalen-1-yl)-N'-alkyl Oxalamide Ligands Enables Cu-Catalyzed Aryl Amination with High Turnovers. *Org. Lett.* **2017**, *19*, 2809–
- (9) Bhunia, S.; De, S.; Ma, D. Room Temperature Cu-Catalyzed N-Arylation of Oxazolidinones and Amides with (Hetero)Aryl Iodides. *Org. Lett.* **2022**, *24*, 1253–1257.
- (10) Job, G. E.; Buchwald, S. L. Copper-Catalyzed Arylation of  $\beta$ -Amino Alcohols. *Org. Lett.* **2002**, *4*, 3703–3706.
- (11) Antilla, J. C.; Baskin, J. M.; Barder, T. E.; Buchwald, S. L. Copper-Diamine-Catalyzed N-Arylation of Pyrroles, Pyrazoles, Indazoles, Imidazoles, and Triazoles. *J. Org. Chem.* **2004**, *69*, 5578–5587.
- (12) Altman, R. A.; Buchwald, S. L. 4,7-Dimethoxy-1,10-phenanthroline: An Excellent Ligand for the Cu-Catalyzed N-Arylation of Imidazoles. *Org. Lett.* **2006**, *8*, 2779–2782.
- (13) Modak, A.; Nett, A. J.; Swift, E. C.; Haibach, M. C.; Chan, V. S.; Franczyk, T. S.; Shekhar, S.; Cook, S. P. Cu-Catalyzed C-N Coupling with Sterically Hindered Partners. ACS Catal. 2020, 10, 10495—10499.

- (14) Barnes, D. M.; Shekhar, S.; Dunn, T. B.; Barkalow, J. H.; Chan, V. S.; Franczyk, T. S.; Haight, A. R.; Hengeveld, J. E.; Kolaczkowski, L.; Kotecki, B. J.; Liang, G.; Marek, J. C.; McLaughlin, M. A.; Montavon, D. K.; Napier, J. J. Discovery and Development of Metal-Catalyzed Coupling Reactions in the Synthesis of Dasabuvir, an HCV-Polymerase Inhibitor. *J. Org. Chem.* **2019**, *84*, 4873–4892.
- (15) Kuethe, J. T.; Childers, K. G.; Humphrey, G. R.; Journet, M.; Peng, Z. A Rapid, Large-Scale Synthesis of a Potent Cholecystokinin (CCK) 1R Receptor Agonist. *Org. Process Res. Dev.* **2008**, *12*, 1201–1208.
- (16) Yang, C.-T.; Fu, Y.; Huang, Y.-B.; Yi, J.; Guo, Q.-X.; Liu, L. Room-Temperature Copper-Catalyzed Carbon-Nitrogen Coupling of Aryl Iodides and Bromides Promoted by Organic Ionic Bases. *Angew. Chem., Int. Ed.* **2009**, *48*, 7398–7401.
- (17) Sung, S.; Sale, D.; Braddock, D. C.; Armstrong, A.; Brennan, C.; Davies, R. P. Mechanistic Studies on the Copper-Catalyzed N-Arylation of Alkylamines Promoted by Organic Soluble Ionic Bases. *ACS Catal.* **2016**, *6*, 3965–3974.
- (18) Lo, Q. A.; Sale, D.; Braddock, D. C.; Davies, R. P. New Insights into the Reaction Capabilities of Ionic Organic Bases in Cu-Catalyzed Amination. *Eur. J. Org. Chem.* **2019**, 2019, 1944–1951.
- (19) Chen, Z.; Ma, D. Cu/N,N'-Dibenzyloxalamide-Catalyzed N-Arylation of Heteroanilines. Org. Lett. 2019, 21, 6874–6878.
- (20) Giri, R.; Hartwig, J. F. Cu(I)—Amido Complexes in the Ullmann Reaction: Reactions of Cu(I)—Amido Complexes with Iodoarenes with and without Autocatalysis by CuI. *J. Am. Chem. Soc.* **2010**, *132*, 15860—15863.
- (21) Sherborne, G. J.; Adomeit, S.; Menzel, R.; Rabeah, J.; Brückner, A.; Fielding, M. R.; Willans, C. E.; Nguyen, B. N. Origins of high catalyst loading in copper(i)-catalysed Ullmann—Goldberg C—N coupling reactions. *Chem. Sci.* **2017**, *8*, 7203—7210.
- (22) Strieter, E. R.; Blackmond, D. G.; Buchwald, S. L. The Role of Chelating Diamine Ligands in the Goldberg Reaction: A Kinetic Study on the Copper-Catalyzed Amidation of Aryl Iodides. *J. Am. Chem. Soc.* **2005**, *127*, 4120–4121.
- (23) Lo, Q. A.; Sale, D.; Braddock, D. C.; Davies, R. P. Mechanistic and Performance Studies on the Ligand-Promoted Ullmann Amination Reaction. *ACS Catal.* **2018**, *8*, 101–109.
- (24) Gurjar, K. K.; Sharma, R. K. Mechanistic Studies of Ullmann-Type C-N Coupling Reactions: Carbonate-Ligated Copper(III) Intermediates. *ChemCatChem* **2017**, *9*, 862–869.
- (25) Tye, J. W.; Weng, Z.; Johns, A. M.; Incarvito, C. D.; Hartwig, J. F. Copper Complexes of Anionic Nitrogen Ligands in the Amidation and Imidation of Aryl Halides. *J. Am. Chem. Soc.* **2008**, *130*, 9971–9983.
- (26) Sambiagio, C.; Marsden, S. P.; Blacker, A. J.; McGowan, P. C. Copper catalysed Ullmann type chemistry: from mechanistic aspects to modern development. *Chem. Soc. Rev.* **2014**, *43*, 3525–3550.
- (27) Shekhar, S.; Ryberg, P.; Hartwig, J. F.; Mathew, J. S.; Blackmond, D. G.; Strieter, E. R.; Buchwald, S. L. Reevaluation of the Mechanism of the Amination of Aryl Halides Catalyzed by BINAP-Ligated Palladium Complexes. *J. Am. Chem. Soc.* **2006**, *128*, 3584–3591.
- (28) Ferretti, A. C.; Brennan, C.; Blackmond, D. G. Reservoir catalysis: Rationalization of anomalous reaction orders in Pd-catalyzed amination of aryl halides. *Inorg. Chim. Acta* **2011**, *369*, 292–295.
- (29) Hoi, K. H.; Çalimsiz, S.; Froese, R. D. J.; Hopkinson, A. C.; Organ, M. G. Amination with Pd NHC Complexes: Rate and Computational Studies Involving Substituted Aniline Substrates. *Chem.—Eur. J.* **2012**, *18*, 145–151.
- (30) Hu, H.; Qu, F.; Gerlach, D. L.; Shaughnessy, K. H. Mechanistic Study of the Role of Substrate Steric Effects and Aniline Inhibition on the Bis(trineopentylphosphine)palladium(0)-Catalyzed Arylation of Aniline Derivatives. *ACS Catal.* **2017**, *7*, 2516–2527.
- (31) Ruiz-Castillo, P.; Blackmond, D. G.; Buchwald, S. L. Rational Ligand Design for the Arylation of Hindered Primary Amines Guided by Reaction Progress Kinetic Analysis. *J. Am. Chem. Soc.* **2015**, *137*, 3085–3092.
- (32) Wilders, A. M.; Henle, J.; Haibach, M. C.; Swiatowiec, R.; Bien, J.; Henry, R. F.; Asare, S. O.; Wall, A. L.; Shekhar, S. Pd-Catalyzed Cross-Coupling of Hindered, Electron-Deficient Anilines with Bulky

- (Hetero)aryl Halides Using Biaryl Phosphorinane Ligands. *ACS Catal.* **2020**, *10*, 15008–15018.
- (33) Ouyang, J.-S.; Liu, S.; Pan, B.; Zhang, Y.; Liang, H.; Chen, B.; He, X.; Chan, W. T. K.; Chan, A. S. C.; Sun, T.-Y.; Wu, Y.-D.; Qiu, L. A Bulky and Electron-Rich N-Heterocyclic Carbene—Palladium Complex (SIPr)Ph2Pd(cin)Cl: Highly Efficient and Versatile for the Buchwald—Hartwig Amination of (Hetero)aryl Chlorides with (Hetero)aryl Amines at Room Temperature. ACS Catal. 2021, 11, 9252—9261.
- (34) Schmidt, O. P.; Dechert-Schmitt, A.-M.; Garnsey, M. R.; Wisniewska, H. M.; Blackmond, D. G. Kinetic Analysis of Catalytic Organic Reactions Using a Temperature Scanning Protocol. *Chem-CatChem* **2019**, *11*, 3808–3813.
- (35) Schmidt, O. P.; Blackmond, D. G. Temperature-Scanning Reaction Protocol Offers Insights into Activation Parameters in the Buchwald—Hartwig Pd-Catalyzed Amination of Aryl Halides. *ACS Catal.* **2020**, *10*, 8926–8932.
- (36) Hoi, K. H.; Organ, M. G. Potassium 2,2,5,7,8-Pentamethylchroman-6-oxide: A Rationally Designed Base for Pd-Catalysed Amination. *Chem.—Eur. J.* **2012**, *18*, 804–807.
- (37) Semeniuchenko, V.; Braje, W. M.; Organ, M. G. Sodium Butylated Hydroxytoluene: A Functional Group Tolerant, Eco-Friendly Base for Solvent-Free, Pd-Catalysed Amination. *Chem.—Eur. J.* **2021**, *27*, 12535–12539.
- (38) Brusoe, A. T.; Hartwig, J. F. Palladium-Catalyzed Arylation of Fluoroalkylamines. *J. Am. Chem. Soc.* **2015**, *137*, 8460–8468.
- (39) Shekhar, S.; Hartwig, J. F. Effects of Bases and Halides on the Amination of Chloroarenes Catalyzed by Pd(PtBu3)2. *Organometallics* **2007**, *26*, 340–351.
- (40) Schulte, J., II; Tweedie, S. R. Palladium-Catalyzed Couplings of Heteroaryl Amines with Aryl Halides Using Sodium Phenolate as the Stoichiometric Base. *Synlett* **2007**, 2007, 2331–2336.
- (41) Olsen, E. P. K.; Arrechea, P. L.; Buchwald, S. L. Mechanistic Insight Leads to a Ligand Which Facilitates the Palladium-Catalyzed Formation of 2-(Hetero)Arylaminooxazoles and 4-(Hetero)-Arylaminothiazoles. *Angew. Chem., Int. Ed.* **2017**, *56*, 10569–10572.
- (42) See Section S2.20 in the Supporting Information for details.
- (43) See Sections S2.19 and S4.7 in the Supporting Information for details.
- (44) See Section S2.21 in the Supporting Information for details.
- (45) Lefèvre, G.; Franc, G.; Tlili, A.; Adamo, C.; Taillefer, M.; Ciofini, I.; Jutand, A. Contribution to the Mechanism of Copper-Catalyzed C—N and C—O Bond Formation. *Organometallics* **2012**, *31*, 7694—7707.
- (46) Zhang, Y.; Yang, X.; Yao, Q.; Ma, D. CuI/DMPAO-Catalyzed N-Arylation of Acyclic Secondary Amines. *Org. Lett.* **2012**, *14*, 3056–3059
- (47) Yu, H.-Z.; Jiang, Y.-Y.; Fu, Y.; Liu, L. Alternative Mechanistic Explanation for Ligand-Dependent Selectivities in Copper-Catalyzed N- and O-Arylation Reactions. *J. Am. Chem. Soc.* **2010**, *132*, 18078–18091.
- (48) Maiti, D.; Buchwald, S. L. Orthogonal Cu- and Pd-Based Catalyst Systems for the O- and N-Arylation of Aminophenols. *J. Am. Chem. Soc.* **2009**, *131*, 17423–17429.
- (49) Altman, R. A.; Anderson, K. W.; Buchwald, S. L. Pyrrole-2-carboxylic Acid as a Ligand for the Cu-Catalyzed Reactions of Primary Anilines with Aryl Halides. *J. Org. Chem.* **2008**, *73*, 5167–5169.
- (50) 3a was formed in 12% yield and 29 in 25% yield using pyrrole-2-carboxylic acid as ligand under the reaction conditions shown in Figure
- (51) Becke, A. D. A new mixing of Hartree–Fock and local density-functional theories. *J. Chem. Phys.* **1993**, *98*, 1372–1377.
- (52) Lee, C.; Yang, W.; Parr, R. G. Development of the Colle-Salvetti correlation-energy formula into a functional of the electron density. *Phys. Rev. B* **1988**, *37*, 785–789.
- (53) Tao, J.; Perdew, J. P.; Staroverov, V. N.; Scuseria, G. E. Climbing the Density Functional Ladder: Nonempirical Meta–Generalized Gradient Approximation Designed for Molecules and Solids. *Phys. Rev. Lett.* **2003**, *91*, No. 146401.
- (54) Marenich, A. V.; Cramer, C. J.; Truhlar, D. G. Universal Solvation Model Based on Solute Electron Density and on a Continuum Model of

- the Solvent Defined by the Bulk Dielectric Constant and Atomic Surface Tensions. J. Phys. Chem. B 2009, 113, 6378–6396.
- (55) See Sections S4.1 and S4.4 in the Supporting Information for details.
- (56) See Sections S4.2 and S4.5 in the Supporting Information for details.
- (57) See Sections S4.2 and S4.6 in the Supporting Information for details.
- (58) See Section S2.5 in the Supporting Information for details
- (59) See Section S2.18 in the Supporting Information for details.
- (60) See Figure S22 in the Supporting Information for details.
- (61) Gui, J.; Pan, C.-M.; Jin, Y.; Qin, T.; Lo, J. C.; Lee, B. J.; Spergel, S. H.; Mertzman, M. E.; Pitts, W. J.; La Cruz, T. E.; Schmidt, M. A.; Darvatkar, N.; Natarajan, S. R.; Baran, P. S. Practical Olefin Hydroamination With Nitroarenes. *Science* **2015**, *348*, 886–891.
- (62) Rucker, R. P.; Whittaker, A. M.; Dang, H.; Lalic, G. Synthesis of Hindered Anilines: Copper-Catalyzed Electrophilic Amination of Aryl Boronic Esters. *Angew. Chem. Int. Ed.* **2012**, *51*, 3953–3956.

#### NOTE ADDED AFTER ASAP PUBLICATION

This paper was originally published ASAP on February 10, 2023. NMR spectra were added to the Supporting Information PDF, and CIF files were uploaded as additional Supporting Information. The corrected version reposted on February 16, 2023

### **□** Recommended by ACS

# Cu(II)/PTABS-Promoted, Regioselective $S_NAr$ Amination of Polychlorinated Pyrimidines with Mechanistic Understanding

Harshita Shet, Anant R. Kapdi, et al.

JULY 24, 2023

THE JOURNAL OF ORGANIC CHEMISTRY

READ 🗹

# Cu/Oxalic Diamide-Catalyzed Coupling of Terminal Alkynes with Aryl Halides

Ying Chen, Dawei Ma, et al.

FEBRUARY 13, 2023

THE JOURNAL OF ORGANIC CHEMISTRY

READ 🗹

## Nickel-Catalyzed Electroreductive Coupling of Alkylpyridinium Salts and Aryl Halides

Jiantao Fu, Dipannita Kalyani, et al.

JUNE 28, 2023 ACS CATALYSIS

READ [7

#### Relay C-H Functionalization Enables De Novo Synthesis of Pyridines and Pyridones

Qing-Peng Liu, Ye Wei, et al.

APRIL 13, 2023

ACS CATALYSIS

READ 🗹

Get More Suggestions >